

## Thermally Rearranged (TR) Poly(ether–benzoxazole) Membranes for Gas Separation

Mariola Calle and Young Moo Lee\*

*WCU Department of Energy Engineering, College of Engineering, Hanyang University, Seoul 133-791, Republic of Korea*

*Received December 17, 2010; Revised Manuscript Received January 6, 2011*

**ABSTRACT:** Thermal rearrangement of hydroxyl-containing polyimides in solid state formed microporous polybenzoxazoles showing extraordinarily fast molecular transport for small gas molecules. Their microporous structure and size distribution can be tuned easily by varying the chemical structure of the precursor hydroxyl–polyimide and by using different thermal treatment protocols. This manuscript reports, for the first time, the synthesis of ether containing polybenzoxazole, that is, poly(ether–benzoxazole) (PEBO) membranes by thermal rearrangement of a novel fluorinated poly(*o*-hydroxy ether–imide). The effect of increased chain flexibility on the physical and transport properties of the resultant thermally rearranged (TR) polymer membranes for different thermal treatment protocols (e.g., final temperature and thermal dwell time) have been examined and reported in detail.

### Introduction

Thermally rearranged polybenzoxazole (TR-PBO) membranes have emerged as a new class of microporous organic materials showing extraordinarily fast molecular transport, as well as molecular sieving effect for small gas molecules.<sup>1,2</sup> Their microporous structure and size distribution results from thermally driven structural rearrangements in the solid state of precursor aromatic polyimides, containing *o*-hydroxy groups, into the highly rigid, ladder-like polybenzoxazole structure. Free volume elements and their size distribution can be tuned easily by varying the monomer structures of the precursor polyimides and by using different thermal treatment protocols. Thus, in our previous studies, the thermal conversion of a series of *o*-hydroxy polyimides prepared from diverse commercially available dianhydrides and bis(*o*-amino phenol)s was carried out and their gas transport behavior was examined by varying the heat treatment protocol.<sup>2–5</sup> Most of these TR polymers showed outstanding gas separation performance, overcoming polymeric upper bounds for gas separation, but strongly dependent on the chemical structure of the precursor polyimides and also on the thermal rearrangement treatment. Thus, TR-PBO membranes containing six bulky fluorine groups, derived from 4,4'-(hexafluoroisopropylidene)diphthalic anhydride (6FDA) and 2,2'-bis(3-amino-4-hydroxyphenyl)hexafluoropropane (bisAPAF) displayed the highest fractional free volumes and permeabilities among all the TR-PBO membranes reported.<sup>1,2</sup> Moreover, as a rule, the gas permeability increased dramatically and the gas selectivity decreased slightly by increasing the heat treatment temperature. Alternatively, size and distribution of free volume cavities created during thermal conversion could be tuned easily by copolymerization. Thus, poly(benzoxazole-*co*-imide) membranes were prepared from the thermal rearrangement of poly(hydroxyl imide-*co*-imide).<sup>3</sup> By varying the composition in the copolymer, it was possible to control the pore volume and surface area in the final TR membrane. In addition, thermally rearranged copolymerization

of stiff and selective pyrrolone and high permeable benzoxazole moieties was a suitable route to enhance gas selectivity of TR-PBO membranes without significant losses in gas permeability.<sup>4</sup> Hence, poly(benzoxazole-*co*-pyrrolone) copolymers in various compositions were synthesized from thermal rearrangement of precursors polyimides containing both hydroxyl and amino groups. On the other hand, the type of imidization of precursor hydroxyl–polyimide also played an important role in TR polymer membranes, resulting in significant deviations in free volume elements; PBO from azeotropic hydroxyl–polyimide without any cross-linking represented the highest density and lowest free volume elements, with permeabilities much smaller than those of other TR-PBO.<sup>5</sup>

These variations in structure–property relationship of TR membranes due to different types of modifications in the precursor polyimide structure, as well as in the thermal rearrangement protocol, prompted us to consider the possibility of tuning the formation of free volume elements in TR-PBO polymers, in terms of temperature and rate of conversion, by increasing the flexibility of the polybenzoxazole backbone. The synthetic modification of the basic rigid PBO chain structure by the introduction of flexibilizing ether linkages along the polymer chain have been reported before. Hence, poly(ether–benzoxazole)s (PEBOs) are generally prepared by step-growth polymerization of aromatic bis(*o*-aminophenol)s with aromatic diacid derivatives, any of them containing ether groups.<sup>6–10</sup> Alternatively, PEBOs have been synthesized by nucleophilic aromatic substitution where the generation of an ether linkage is the polymer-forming reaction.<sup>11</sup> In all cases, the presence of ether connecting groups enhanced the tractability and tensile properties of conventional PBOs, without any impairment in the high thermal stability characteristic of these heteroaromatic polymers.

As a continuation on the study and development of new high free volume polymer membrane materials using the thermal rearrangement concept, here we describe for the first time the synthesis and characterization of poly(ether–benzoxazole) membranes by thermal rearrangement of a novel fluorinated ether-containing poly(*o*-hydroxy imide) (HPEI). The effect of increased

\*Corresponding author. Telephone: +82-2-2220-0525. Fax: +82-2-2291-5982. E-mail: ymlee@hanyang.ac.kr.

chain flexibility on the physical and transport properties of the resultant TR polymer membranes for different thermal treatment protocols (e.g., final temperature and thermal dwell time) have been examined and reported in detail.

## Experimental Section

**Materials.** Solvents and reactants were of reagent-grade quality and used without further purification. 5-Fluoro-2-nitrophenol, hydrazine monohydrate, and palladium 10 wt % on activated carbon were purchased from Aldrich and 4,4'-(Hexafluoroisopropylidene)diphenol, to Alfa Aesar. 4,4'-Hexafluoroisopropylidene diphthalic anhydride (6FDA) was purchased from Daikin Industries, Ltd. (Osaka, Japan), and it was sublimed just before being used.

**Monomer synthesis.** The ether-containing bis(*o*-aminophenol) monomer, 2,2-Bis(4-(4-amino-3-hydroxyphenoxy)phenyl)-hexafluoropropane (6FBAHPP), was synthesized in two steps, according to the previously reported method,<sup>12</sup> from 4,4'-(hexafluoroisopropylidene)diphenol and 5-fluoro-2-nitrophenol by nucleophilic aromatic substitution in the presence of potassium carbonate (K<sub>2</sub>CO<sub>3</sub>) and DMF as solvent, followed by catalytic reduction with hydrazine hydrate and Pd/C as catalyst. The crude product was recrystallized from a mixed solution (ethanol:water = 2:1, v/v) under nitrogen atmosphere. Elemental analysis and <sup>1</sup>H NMR spectroscopic techniques were used to identify the structures of the intermediate dinitro compound and the final hydroxyl diamine monomer, which were in good agreement with the previous literature.<sup>12</sup> 2,2-Bis(4-(3-hydroxy-4-nitrophenoxy)phenyl)hexafluoropropane. Anal. Calcd for C<sub>27</sub>H<sub>16</sub>F<sub>6</sub>N<sub>2</sub>O<sub>8</sub>: C, 53.11; H, 2.62; N, 4.59. Found: C, 52.95; H, 2.22; N, 4.62. <sup>1</sup>H NMR (300 MHz, DMSO-*d*<sub>6</sub>): 11.30 (s br, 2H) 7.99 (d, 2H, *J* = 8.8 Hz), 7.45 (d, 4H, *J* = 9.0 Hz), 7.27 (d, 4H, *J* = 9.0 Hz), 6.64 (d, 2H, *J* = 2.5 Hz), 6.60 (dd, 2H, *J* = 2.5 Hz, *J* = 8.8 Hz). 2,2-Bis(4-(4-amino-3-hydroxyphenoxy)phenyl)-hexafluoropropane. Anal. Calcd For C<sub>27</sub>H<sub>20</sub>F<sub>6</sub>N<sub>2</sub>O<sub>4</sub>: C, 58.91; H, 3.64; N, 5.09. Found: C, 58.50; H, 3.52; N, 4.98. <sup>1</sup>H NMR (300 MHz, DMSO-*d*<sub>6</sub>): 9.18 (s br, 2H) 7.22 (d, 4H, *J* = 8.8 Hz), 6.90 (d, 4H, *J* = 8.8 Hz), 6.57 (d, 2H, *J* = 8.2 Hz), 6.39 (d, 2H, *J* = 2.5 Hz), 6.32 (dd, 2H, *J* = 2.5 Hz, *J* = 8.2 Hz) 4.50 (s br, 4H).

**Poly(ether *o*-hydroxyimide) (HPEI) Synthesis.** A three-necked flask, equipped with a mechanical stirrer and gas inlet and outlet, was charged with 10.0 mmol of diamine and 10.0 mL of NMP. The mixture was stirred at room temperature under a blanket of nitrogen until the solid was entirely dissolved. Then, the solution was cooled to 0 °C, and 6FDA dianhydride (10.0 mmol) was added, followed by 10.0 mL of NMP. The reaction mixture was stirred for 15 min at 0 °C; then, the temperature was raised to room temperature and left overnight. *o*-Xylene (30 mL) as an azeotropic agent was then added to the solution, which was stirred vigorously and heated for 6 h at 180 °C to promote imidization. During this step, the water released by the ring-closure reaction was separated as a xylene azeotrope. The resulting brown-colored solution was cooled to room temperature, precipitated in distilled water, washed several times with water and dried in a convection oven at 120 °C for 12 h. <sup>1</sup>H NMR (300 MHz, DMSO-*d*<sub>6</sub>): 10.18 (s, 2H, OH), 8.15 (d, 2H, *J* = 8.2 Hz), 7.96 (d, 2H, *J* = 8.2 Hz), 7.75 (s, 2H), 7.40 (d, 4H, *J* = 8.2 Hz), 7.30 (d, 2H, *J* = 8.8 Hz), 7.20 (d, 4H, *J* = 8.8 Hz), 6.65 (d, 2H, *J* = 8.8 Hz), 6.63 (s, 2H). FT-IR (film): ν(–OH) at 3371 cm<sup>–1</sup>, imide ν(C=O) at 1785 and 1715 cm<sup>–1</sup>, imide ν(C–N) at 1390 cm<sup>–1</sup>. Molecular weight: *M*<sub>w</sub> = 97 200, *M*<sub>n</sub> = 21 300 with a polydispersity of 4.2.

**Polyimide Film Formation and Thermal Conversion to Poly(ether–benzoxazole).** The casting of the polyimide was done from a 15 wt % filtered solution in NMP onto a clean glass plate. Cast film was placed in a vacuum oven and heated slowly to 250 °C with holds for 1 h at 100, 150, and 200 °C to evaporate the solvent under high vacuum. The solid film was taken off from the glass plate, rinsed with deionized water, and dried at 120 °C

until the residual solvent and water were removed. The defect-free and clean membrane was cut into 3 cm × 3 cm size strips and placed between quartz plates to prevent film deformation at elevated temperature in a muffle furnace. Each sample was heated to 300 °C at a rate of 5 °C/min, soaked for 1 h, heated further to 400 or 450 °C and maintained for 1 h (or 2 and 3 h) in a high-purity argon atmosphere, following the literature.<sup>1–5</sup> After thermal treatment, the furnace was slowly cooled to room temperature, and the brown-colored membranes were stored in a desiccator.

**Measurements.** <sup>1</sup>H spectra were recorded on a Mercury Plus 300 MHz spectrometer (Varian, Inc., Palo Alto, CA). The attenuated total reflection Fourier transform infrared (ATR-FTIR) spectra of samples were measured using an Infrared Microspectrometer (IlluminatIR, SensIR Technologies, Danbury, CT). Elemental analysis were performed with a Thermofinnigan EA1108 (Fisons Instrument Co., Italy) elemental analyzer. Molecular weight of precursor polyimide was measured by gel permeation chromatography (GPC, Tosoh HLC-8320 GPC, Tokyo, Japan) with a TSK SuperMultipore HZ-M column and a refractive index (RI) detector in THF on the basis of standard polystyrenes. Differential scanning calorimetry (DSC) analyses were performed on a TA Instruments Q-20 calorimeter at a heating rate of 20 °C/min under nitrogen. Thermogravimetric analyses (TGAs) were performed on a TA Q-500 thermobalance (TA Instruments, New Castle, DE), coupled with mass spectroscopy (MS) ThermoStar GSD 301T (Pfeiffer Vacuum GmbH, Asslar, Germany).

Wide angle X-ray diffractometry (WAXD) were recorded in the reflection mode at room temperature by using a Rigaku Denki D/MAX-2500 (Rigaku, Japan) diffractometer. Cu Kα (wavelength λ = 1.54 Å) radiation was used. The average *d*-spacing value was determined from Bragg's equation in the 2 theta range of 5–50° with a scan rate of 5°/min. Fractional free volume (FFV, *V*<sub>f</sub>), was calculated from the densities measured by a Sartorius LA 120S (Sartorius AG, Goettingen, Germany) balance with a density kit by a buoyancy method as follows:

$$V = \frac{M_0}{\rho} \quad (1)$$

$$V_f = \frac{V - 1.3 \times V_w}{V} \quad (2)$$

where *V* is the molar volume of polymers (mol cm<sup>3</sup>/mol) derived from density, and *V*<sub>w</sub> is the van der Waals molar volume based on Bondi's group contribution theory.

Gas permeation properties were obtained from a custom-made instrument using the time-lag method as described in our previous studies.<sup>13</sup> For six kinds of small gas molecules, He (2.6 Å), H<sub>2</sub> (2.89 Å), CO<sub>2</sub> (3.3 Å), O<sub>2</sub> (3.46 Å), N<sub>2</sub> (3.64 Å), and CH<sub>4</sub> (3.8 Å), pressure increase through the membrane in a fixed downstream chamber were acquired from 0 to 10 mmHg against 760 mmHg of upstream pressure. From the slopes and intercepts in a steady state region of pressure increment as a function of time, gas permeability coefficients were calculated by using the following equation:

$$P = \left( \frac{V \cdot T_0 \cdot l}{p_0 \cdot T \cdot \Delta p \cdot A} \right) \frac{dp}{dt} \quad (4)$$

where *P* (Barrer) is the gasmembrane thickness, Δ*p* (cmHg) is the pressure difference between upstream and downstream, *T*(K) is the measurement temperature, *A* (cm<sup>2</sup>) is the effective membrane area, *p*<sub>0</sub> and *T*<sub>0</sub> are the standard pressure and temperature, and *dp/dt* is the rate of the pressure rise at steady state. The ideal selectivity (α<sub>1/2</sub>) for components 1 and 2 was defined as the ratio of gas permeability of the two components.

Scheme 1. Synthesis of Thermally Rearranged Poly(ether–benzoxazole) (TR-PEBO)

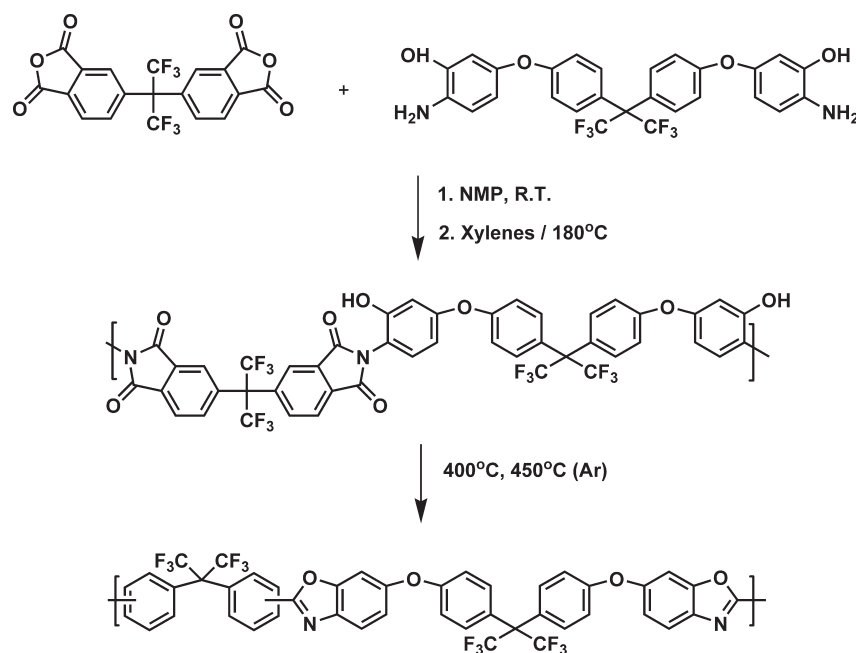


Table 1. Elemental Analysis of Precursor Polyimide and Poly(ether–benzoxazole) Membranes

sample	molecular formula of repeating unit	C (wt %)	H (wt %)	N (wt %)
HPEI	C <sub>46</sub> H <sub>22</sub> N <sub>2</sub> O <sub>8</sub> F <sub>12</sub>	56.23 (57.63) <sup>a</sup>	2.11 (2.31) <sup>a</sup>	2.80 (2.92) <sup>a</sup>
400–1	C <sub>44</sub> H <sub>22</sub> N <sub>2</sub> O <sub>4</sub> F <sub>12</sub>	60.03 (60.70) <sup>a</sup>	2.02 (2.55) <sup>a</sup>	3.08 (3.22) <sup>a</sup>
400–2	C <sub>44</sub> H <sub>22</sub> N <sub>2</sub> O <sub>4</sub> F <sub>12</sub>	61.73 (60.70) <sup>a</sup>	2.73 (2.55) <sup>a</sup>	3.18 (3.22) <sup>a</sup>
400–3	C <sub>44</sub> H <sub>22</sub> N <sub>2</sub> O <sub>4</sub> F <sub>12</sub>	60.53 (60.70) <sup>a</sup>	2.01 (2.55) <sup>a</sup>	3.12 (3.22) <sup>a</sup>
450–1	C <sub>44</sub> H <sub>22</sub> N <sub>2</sub> O <sub>4</sub> F <sub>12</sub>	62.90 (60.70) <sup>a</sup>	2.29 (2.55) <sup>a</sup>	3.28 (3.22) <sup>a</sup>
450–2	C <sub>44</sub> H <sub>22</sub> N <sub>2</sub> O <sub>4</sub> F <sub>12</sub>	63.15 (60.70) <sup>a</sup>	1.90 (2.55) <sup>a</sup>	3.25 (3.22) <sup>a</sup>
450–3	C <sub>44</sub> H <sub>22</sub> N <sub>2</sub> O <sub>4</sub> F <sub>12</sub>	65.38 (60.70) <sup>a</sup>	1.83 (2.55) <sup>a</sup>	3.32 (3.22) <sup>a</sup>

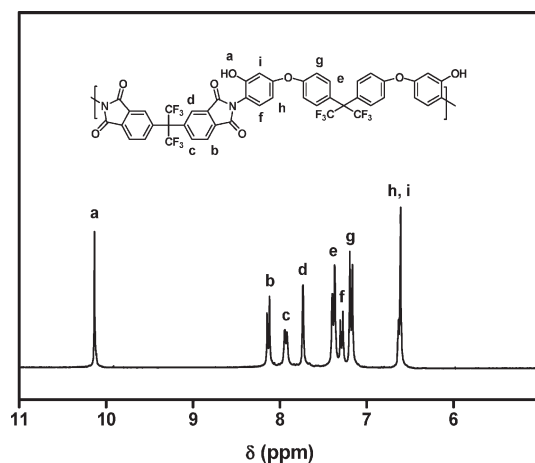
<sup>a</sup>Theoretical values.

## Results and Discussion

**Monomer Synthesis.** The ether-containing bis(*o*-aminophenol) monomer, 2,2-Bis(4-(4-amino-3-hydroxyphenoxy)phenyl)hexafluoropropane (6FBAHPP) was synthesized in two steps, by potassium carbonate mediated nucleophilic substitution reaction of 5-fluoro-2-nitrophenol with 4,4'-(hexafluoroisopropylidene)diphenol, followed by catalytic reduction with hydrazine hydrate and Pd/C as catalyst. Elemental analysis and <sup>1</sup>H NMR spectroscopic techniques were used to identify the structures of the intermediate dinitro compound and the final hydroxyl diamine monomer, which were in good agreement with the previous literature.<sup>12</sup>

**Synthesis and Characterization of Precursor Polyimide.** The novel-fluorinated hydroxy–poly(ether–imide) was synthesized from bis(*o*-aminophenol) (6FBAHPP) and 6FDA dianhydride by a two step polyimidation method by poly(ether–amic acid) intermediate (Scheme 1). In the second stage, *o*-xylene as an azeotropic agent was added to the polymer solution, which was stirred vigorously and heated for 6 h at 180 °C to promote imidization. During this step, the water released by the ring-closure reaction was separated as a xylene azeotrope.

The final poly(ether–imide) (HPEI) thus obtained showed an inherent viscosity of 0.70 dL/g, with weight-average molecular weight and polydispersity of 97 200 and 4.2, respectively, as determined by GPC in THF solvent. The elemental analysis values of HPEI listed in Table 1 were in good agreement for carbon, hydrogen and nitrogen.

Figure 1. <sup>1</sup>H NMR (DMSO-*d*<sub>6</sub>, 300 MHz) spectrum of precursor poly(ether–imide) (HPEI).

Its chemical structure was confirmed by <sup>1</sup>H NMR and IR spectroscopies. The <sup>1</sup>H NMR spectrum is showed in Figure 1.

The IR spectrum supported the complete imidation (Figure 2); characteristic absorption bands of polyimides appeared at 1785 (b: asym C=O str), 1715 (c: sym C=O str), 1390 (d: C–N str), whereas no signals associated with polyamic acid were observed. In addition, the broad band around 3400 cm<sup>−1</sup> is assigned to the hydroxyl group (a), and the



strong absorption in the region of 1150–1250  $\text{cm}^{-1}$  can be attributed to the C–O and C–F stretching.

Glass transition temperature ( $T_g$ ) was determined by DSC (Table 2). As expected, the presence of ether connecting groups greatly affected the mobility of the chains, and so, the  $T_g$  of poly(ether-imide) (**HPEI**) is 280  $^{\circ}\text{C}$ , whereas for the related hydroxy-polyimide without ether linkages (6FDA-APAF) (from 4,4'-hexafluoroisopropylidene diphthalic anhydride (6FDA) and 2,2'-bis(3-amino-4-hydroxyphenyl)hexafluoropropane diamine (bis-APAF)) is 300  $^{\circ}\text{C}$ , as previously reported.<sup>5</sup> The effect of flexible ether moieties in the polymer backbone can also be seen when testing the mechanical properties (Table 2); **HPEI** films had tensile strength of 97 MPa and elongation at break of around

12%, about 4 times higher than the elongation described for typical 6FDA-APAF polyimide (3.1%).<sup>1</sup>

**Thermal Rearrangement of poly(ether *o*-hydroxyimide) (**HPEI**) into Poly(ether-benzoxazole) (**PEBO**).** Before thermal treatment, thermal behavior of **HPEI** precursor was investigated by TGA-MS to elucidate thermal conversion characteristics and to set up proper thermal treatment conditions. As was previously well-demonstrated,<sup>1,2,5,14,15</sup> the thermal rearrangement of *o*-hydroxy-imides to benzoxazoles accompanies the evolution of carbon dioxide. Thus, the thermogram of **HPEI** (Figure 3) showed two distinct weight losses; the conversion to **PEBO** in the range 330–470  $^{\circ}\text{C}$ , where the amount of  $\text{CO}_2$  evolution reached the maximum value at around 400  $^{\circ}\text{C}$  as confirmed by simultaneous mass spectroscopy, and the generalized decomposition of the polymer backbone around 500–600  $^{\circ}\text{C}$ . Hence, from this thermogravimetric analysis, we adopted the conditions to accomplish the rearrangement of this newly synthesized poly(ether *o*-hydroxyimide) (**HPEI**) to poly(ether-benzoxazole) (**PEBO**) in the solid state. In this work we intend to focus on the effect of thermal treatment conditions on the rearrangement ratio and properties of **TR-PEBO** membranes. Two different treatment temperatures were selected for this purpose: 400  $^{\circ}\text{C}$ , maximum amount of  $\text{CO}_2$  evolution temperature, and 450  $^{\circ}\text{C}$ , final weight loss temperature. Moreover, the influence of different treatment times was also studied, that is, 1, 2, or 3 h heating time.

**PEBO Conversion Study through ATR-FTIR Analysis.** The chemical or structural changes occurring in the films during the thermal treatment were monitored using ATR-FTIR analysis. Defect-free and clean pieces of **HPEI** membrane (previously treated at 300  $^{\circ}\text{C}$  for 1 h) were ramped at 5  $^{\circ}\text{C}/\text{min}$  in a muffle furnace, and held at 400 or 450  $^{\circ}\text{C}$  for 1, 2, or 3 h under a high-purity argon atmosphere. The infrared spectra of these samples and **HPEI** precursor are shown in Figure 2. The formation of the benzoxazole ring-structure from **HPEI** can be easily followed by IR spectroscopy as several distinct changes occur during the thermal treatment; the characteristic O–H stretch at 3400  $\text{cm}^{-1}$  for this hydroxy-containing polyimide (upper spectrum) disappeared in the film sample heated at 400  $^{\circ}\text{C}$  for 1 h (**400-1**), and two distinct peaks at wavenumbers 1475  $\text{cm}^{-1}$  (e) and 1054  $\text{cm}^{-1}$  (f) appeared typical of the benzoxazole ring. However, symmetric and asymmetric carbonyl stretches at 1785 and 1715  $\text{cm}^{-1}$  were still visible, indicating that some imide linkages still remain in the sample. By increasing the treatment time up to 2 h (**400-2**), only a small carbonyl absorbance remains at 1715  $\text{cm}^{-1}$ , that finally becomes imperceptible when heating for 3 h (**400-3**). The rearrangement ratio seems to be also greatly affected by the choice of the treatment temperature and thus, no carbonyl imide peaks were detected for the 450  $^{\circ}\text{C}$  2 and 3 h treated samples (**450-2** and **450-3** respectively) while a very small peak remains in **450-1**. Generally, when a polymer is thermally treated, the

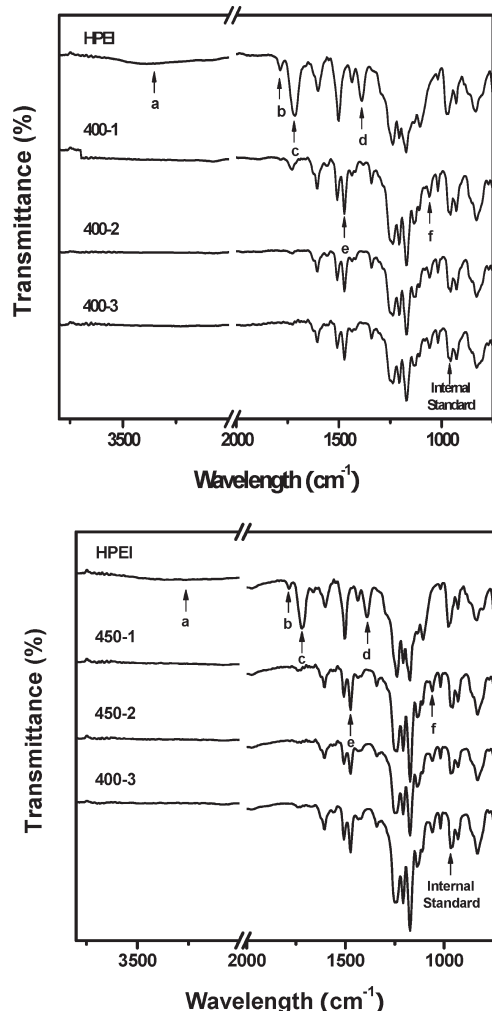


**Figure 2.** ATR-FTIR spectra of **HPEI** precursor and **TR-PEBO** membranes treated at 400 and 450  $^{\circ}\text{C}$  different heating times.

**Table 2.** Thermal and Mechanical Properties of Precursor Polyimide and Poly(ether-benzoxazole) Membranes

sample	$T_g$ ( $^{\circ}\text{C}$ ) <sup>a</sup>	$T_{d(5\%)}$ ( $^{\circ}\text{C}$ ) <sup>b</sup>	char yield (%) <sup>d</sup>	tensile strength (MPa)	elongation at break (%)
<b>HPEI</b>	280	395 <sup>c</sup>	50.5	97	12.3
<b>400-1</b>	243	525	55.3	81	7.3
<b>400-2</b>	239	529	56.6	84	6.5
<b>400-3</b>	242	525	55.7	83	7.1
<b>450-1</b>	250	525	55.0	54	4.0
<b>450-2</b>	311	529	57.4		e
<b>450-3</b>	f	532	60.7	e	e

<sup>a</sup> Middle point of the endothermic step during the second scan of DSC measurements conducted with a heating rate of 20  $^{\circ}\text{C}/\text{min}$  under a nitrogen atmosphere. <sup>b</sup> 5% weight loss temperature in TGA at 10  $^{\circ}\text{C}/\text{min}$  heating rate under a nitrogen atmosphere. <sup>c</sup> Onset of the thermal conversion reaction.

<sup>d</sup> Residual yield in TGA at 800  $^{\circ}\text{C}$  under a nitrogen atmosphere. <sup>e</sup> Brittle films. <sup>f</sup> Not detected.

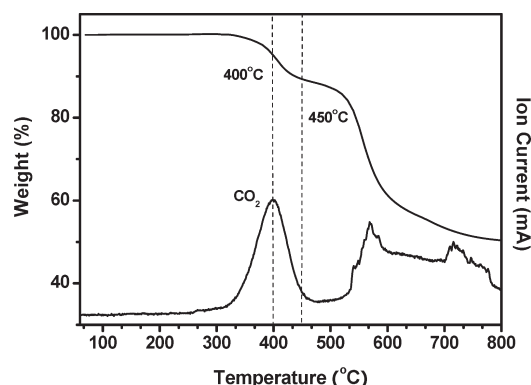


**Figure 3.** Thermogravimetric analysis combined with mass spectroscopy (TG-MS) of HPEI precursor.

absorption intensity of specific groups decrease and a widening of bands are produced upon heating, due to the conversion of the polymer to a carbon structure.<sup>16</sup> However, in our case, all **TR-PEBO** membranes showed well-defined absorption intensities and band wideness, irrespective of the thermal treatment protocol, meaning that no degradation or conversion to a carbon structure is taking place on increasing the intensity of the treatments.

The percent conversion (cyclization or percent ring closure) achieved in these thermally rearranged **PEBO** membranes was estimated by FTIR analysis using eq 1<sup>17</sup>

$$\% \text{ conversion} = \frac{(A_{1054}/A_{\text{internal standard}})_{\text{sample}}}{(A_{1054}/A_{\text{internal standard}})_{\text{std. sample}}} \times 100$$

where  $A_{1054}$  is the absorbance attributed to the benzoxazole ring formation (C–O–C benzoxazole ring stretching) that was normalized by an internal standard ( $A_{\text{internal standard}}$ ) corresponding to the absorbance at  $963 \text{ cm}^{-1}$  (C–H bending of the aromatic ring), which was relatively unaffected by the thermal rearrangement process (remain constant).

As mentioned above, the thermal conversion reaction to **PEBO** from **HPEI** was very sensitive to the reaction temperature. At 400 °C, 90% and 96% of benzoxazole moiety were formed in 1 and 2 h, respectively, whereas complete conversion was achieved after 3 h. Nevertheless, 1 h at 450 °C is enough to reach 95% percent conversion, while overpassing this time 100% of **PEBO** formation is obtained. These results are consistent with other studies, which have shown acceleration in thermal rearrangement kinetics to **PBO** by increasing temperature.<sup>18</sup> Furthermore, they are also in good agreement with Tullios and his colleagues' findings:<sup>15</sup> the more flexible hydroxy-containing polyimides, with lower glass transition temperature, undergo thermal conversion at a faster rate and lower temperature. Hence, they observed that the rigid BPDA-HAB polyimide, arising from 3,3'-dihydroxybiphenyl diamine (HAB) and 3,3',4,4'-bisphenyltetracarboxylic dianhydride (BPDA), required heating for 1 h at 500 °C under nitrogen for near complete conversion to polybenzoxazole whereas heating for 1 h at 400 °C resulted in only slight conversion. This is not the case for the newly synthesized poly(ether imide) **HPEI**, whose improved molecular mobility allows for rearrangement and decarboxylation to occur efficiently at 400 °C. FTIR analysis thus provided a semiquantitative estimate of the percent conversion (effectiveness of the thermal rearrangement) in the **PEBO** films as a function of thermal treatment conditions.

**Characterization of Thermally Rearranged Poly(ether-benzoxazole) (TR-PEBO) Membranes.** To help ascertain the chemical structure of the resultant thermally rearranged

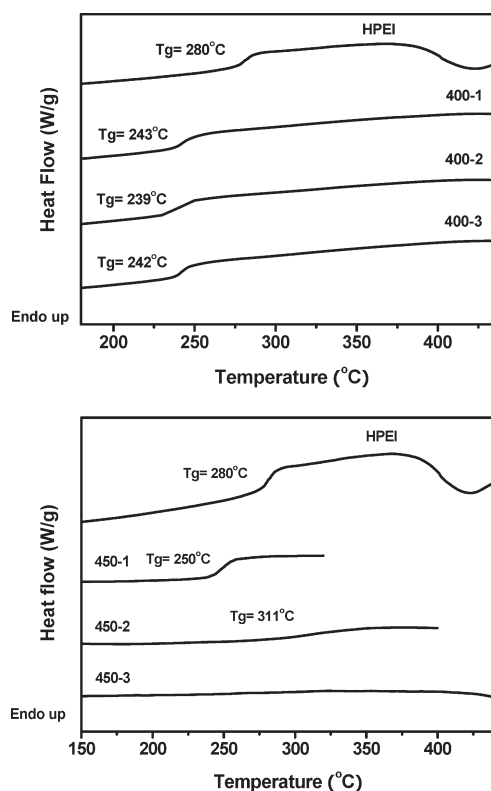


**Figure 4.** Glass transition temperature of **HPEI** precursor and **TR-PEBO** membranes treated at 400 and 450 °C different heating times.

**PEBO** membranes from poly(ether-imide) **HPEI**, elemental analysis was also carried out (Table 1). Thus, the mass ratio of each element showed good correspondence for all the samples treated at 400 °C, that is, **400-1**, **400-2** and **400-3**, whereas samples treated at 450 °C (**450-1**, **450-2**, and **450-3**), showed a small deviation compared to theoretical values, probably due to the more severe conditions when working at this temperature.

The thermal resistance of these **TR-PEBO** membranes was investigated by TGA in  $\text{N}_2$  atmosphere (Table 2). All **TR-PEBO** membranes showed a one-step pattern with 5% weight loss temperature around 525 °C, somewhat higher than the corresponding precursor (**HPEI**) (weight loss considered for the second step), which indicated that thermal rearrangement yielded more thermally stable membranes thanks to benzoxazole ring formation. It should be also pointed out that the modification of the basic rigid polybenzoxazole structure by introduction of flexibilizing linkages does not seem to greatly impair the thermal stability, when compare with related fluorinated **TR-PBO** membranes reported before.<sup>2,5</sup> On the other hand, the residues remaining at 800 °C (char residue) increased slightly when heat-treatment time raised for the samples heated at 450 °C, which can be associated with a higher degree of thermal-cross-linking.

Thermal conversion temperature and time greatly affect the polymer segmental mobility. Thus, as seen in Figure 4 and in Table 2, poly(ether-imide) precursor (**HPEI**) showed a discernible glass transition at 280 °C, followed by a strong and broad exothermic peak around 400–450 °C that was attributed to the intramolecular cyclization to the carboxybenzoxazole intermediate followed by decarboxylation to the final **PEBO**, mechanism widely reported before.<sup>14,15</sup> Beyond our expectations, the conversion to poly(ether-benzoxazole) brings about a significant drop in the glass

Table 3. Physical Properties of Precursor Polyimide and Poly(ether–benzoxazole) Membranes

sample	density (g/cm <sup>3</sup> )	molar volume (cm <sup>3</sup> /g)	fractional free volume (FFV)	increment in FFV (%)	d-spacing (nm)
<b>HPEI</b>	1.451	0.689	0.151		0.59
<b>400–1</b>	1.398	0.715	0.174	15.23	0.63
<b>400–2</b>	1.389	0.720	0.180	19.20	0.62
<b>400–3</b>	1.407	0.710	0.169	11.92	0.62
<b>450–1</b>	1.391	0.719	0.178	17.88	0.66
<b>450–2</b>	1.365	0.733	0.194	28.48	0.66
<b>450–3</b>	1.342	0.745	0.207	37.08	0.66

transition temperature. Thus, the  $T_g$ s of samples heated at 400 °C are around 240 °C, meaning a reduction of about 40 °C regarding hydroxy poly(ether–imide) precursor (**HPEI**). This phenomena had been previously observed by other authors,<sup>8</sup> and it is probably attributable to the less polar nature of benzoxazole rings in comparison with that of imide rings, but also to the reduced intermolecular attractions between polymer chains due to the absence of hydroxy groups in the final **PEBO** structure. Furthermore, these  $T_g$  values are comparable with the glass transition temperature reported by Hedrick et al.<sup>11</sup> for a fluorinated poly(aryl ether–benzoxazole) isomer ( $T_g$  = 241 °C), prepared by nucleophilic aromatic substitution as the polymer forming reaction. Additionally, thermal treatment at 450 °C and eventual cross-linking, as a function of heating time, had a noticeable repercussion on the polymer morphology. Hence, the  $T_g$  of sample **450–1** is 250 °C, whereas for the 2 h thermally treated (**450–2**) went up to 311 °C. Besides, no  $T_g$  inflection below 450 °C was detected for **450–3**, supporting the higher degree of thermal-cross-linking for this membrane.

Heat-treatment temperature greatly affects **TR-PEBO** films properties and characteristics as well. The mechanical properties of **TR-PEBO** films are summarized in Table 2. Thermal rearrangement at 450 °C resulted in slight embrittlement of the films, and so we were not able to evaluate the mechanical properties for the samples **450–2** and **450–3**. However, **TR-PEBO** membranes treated at 400 °C resulted in good quality films, with tensile strengths slightly above 80 MPa and elongation at break around 7%, whereas for **450–1**, the values were somewhat lower. These values of tensile strengths and elongation at break are lower as compared with poly(ether *o*-hydroxy imide) (**HPEI**) precursor, but comparable with previously reported **PEBO** obtained by cyclodehydration of poly(*o*-hydroxyamide)s precursors also in the solid state.<sup>7,10</sup> Therefore, this deteriorating effect on the mechanical properties of **PEBO** films may be attributed on the one hand, to the reducing intermolecular interaction through hydrogen bonding because of the absence of the hydroxyl groups, and on the other hand, to the stress buildup and chain shrinkage upon thermal rearrangement. Nevertheless, it is worth noting the enhancement in the elongation at break, when compared with thermally rearranged polybenzoxazoles previously described, that displayed values around 3–4%;<sup>1</sup> the incorporation of flexibilizing ether linkages resulted in **TR** polybenzoxazoles with improved mechanical property.

The density of the films were measured by a buoyancy method. In all cases, the values for **TR-PEBO** membranes were lower than that for **HPEI** precursor (see Table 3).

It has been well reported that thermal rearrangement of *o*-hydroxypolyimides to polybenzoxazoles in the solid state results in an outstanding enhancement in free volume along with a significant decrease in the density of the **TR-PBOs**.<sup>1,2,5</sup> As a matter of fact, the density of **HPEI** precursor, 1.451 g cm<sup>-3</sup>, diminished as thermal rearrangement proceeded at 400 °C for 1 and 2 h, but unexpectedly, 3 h heat-treatment

lead to an augment of density, even though 100% conversion to **PEBO** was reached at that point. Against it was observed for previously described **TR-PBOs**, the thermal rearrangement to poly(ether benzoxazole) did not imply the generation of a much more stiff polymer structure,<sup>1,2,5</sup> as confirmed from the reduction in the  $T_g$  values. Probably, the presence of flexible ether bonds allows large intrachain, indiscriminant torsional rotation, leading to a rather flexible polybenzoxazole structure. As a result, considering that the treatment temperature of 400 °C is above the glass transition, any physical changes (e.g., the formation of microvoids due to segmental rearrangement and chain disruption) after the thermal conversion could be reversible due to the polymer chains relaxation to repack the created cavities. This fact could explain the increased density for **400–3** membrane. As discussed above, augmenting the rearrangement temperature up to 450 °C, induced the cross-linking of polymer chains, and so, increased the glass transition temperature as a function of heating time. It is known that thermal cross-linking reactions can lead to a higher packing density.<sup>19,20</sup> This was not the case for the samples **450–1**, **450–2**, and **450–3**, that exhibited reduced densities in comparison to 400 °C treated films. This behavior is in agreement with that described in our earlier observation for related **TR-PBOs**, prepared from thermally imidized hydroxyl-containing polyimides,<sup>1</sup> whose cavities increased in size at higher treatment temperatures. Furthermore, the trend was  $\rho(\mathbf{450-3}) > \rho(\mathbf{450-2}) > \rho(\mathbf{450-1})$ , meaning that the longer the heating, the lower the density. Probably, the enhancement in the cross-linking of polymer chains turned out to reduce molecular chain relaxation, and so, the microvoids formed remained more efficiently after conversion, in contrast with that observed for membranes treated at 400 °C, particularly for the **400–3** sample. The smaller density of the polymer corresponds to larger free volume elements. In order to confirm this assumption, fractional free volume (FFV) of all **TR-PEBO** membranes and its precursor were estimated (Table 3). Thus, the calculated FFV value of **HPEI** is 0.151, which falls within the experimentally reported values for polyimides, usually in the range 0.1–0.2.<sup>21</sup> As thermal rearrangement proceeded at different temperatures and times, the FFV raised accordingly with the drop in the density values. Thus, **450–3** showed the highest FFV (0.207), indicating an increase of 37% when compared to **HPEI**. In contrast, the same heating-time, but at lower temperature (**400–3**) accompanied the smallest rise in FFV (about 12%), probably because of compaction of the polymer chains, as pointed out above.

Recently, it has been reported the physical properties and gas transport behaviors of fluorinated **TR-PBOs** prepared by diverse imidization routes.<sup>5</sup> The differences in FFV between precursors and the **TR-polymers** are in the range 29–96%, the smallest value corresponding to **PBO** from azetropic hydroxyl–polyimide. In all cases, the thermal treatment adopted was 450 °C for 1 h. In our case, the sample treated at 450 °C for 1 h, **450–1**, showed an enlargement of only 18% in FFV. The reason for this diminished

efficiency of free volume elements formation for **TR-PEBOs** may reside in the higher degree of flexibility and conformational freedom of the polymer backbone, as a consequence of the presence of ether connecting groups. It seems that with the lower glass transition temperature and much higher mobility for **TR-PEBO** polymer membranes, nonequilibrium conditions are much more difficult to achieve as thermal rearrangement takes place quite above the  $T_g$ , resulting in broader pore size distributions. With the much higher glass transition temperature of the previously reported **TR-PBO** membranes, the TR process occurs near the  $T_g$  and nonequilibrium pore size develops yielding much narrower distributions resulting in more molecular sieving structures.

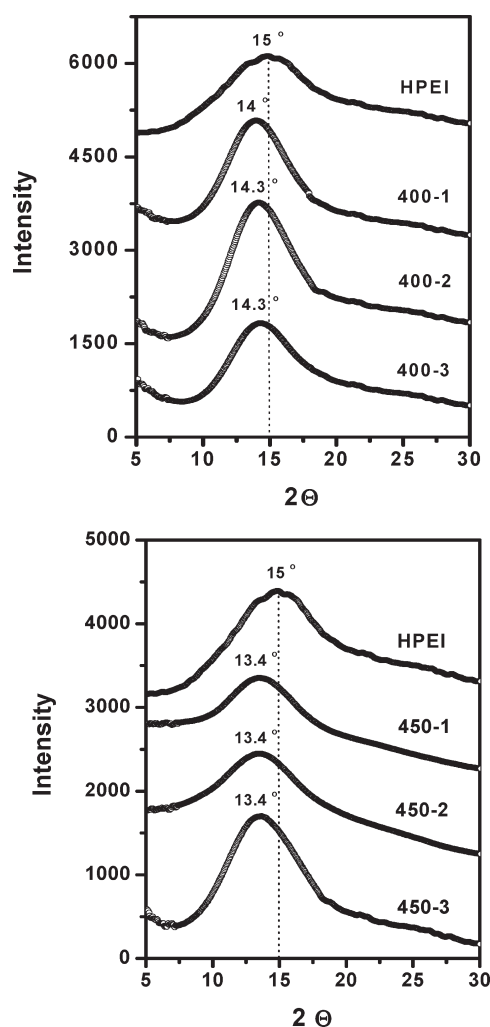


**Figure 5.** Wide angle X-ray diffraction (WAXD) patterns of **HPEI** precursor and **TR-PEBO** membranes treated at 400 and 450 °C different heating times.

While cross-linking occurs during the thermal rearrangement, the nonequilibrium pore size is locked in if the rearrangement takes place near the  $T_g$ . The TR process is thus closer to producing molecular sieving pore sizes if it is conducted at, near or below the  $T_g$ .

Figure 5 compares the X-ray diffraction patterns measured at room temperature, of **TR-PEBO** membranes and **HPEI** precursor. A broad amorphous halo was observed for all the samples, proving the amorphous nature of all these polymers. It is known that the position of the halo maximum can be considered as an indicator of the most probable intersegmental distance ( $d$ -spacing) between the chains, as calculated from Bragg equation. As shown in Figure 5, the position of the amorphous halo maximum at 15° ( $2\theta$ ) for **HPEI** corresponds to a preferential intersegmental distance of 0.59 nm. In all cases, thermal rearrangement to **PEBO** resulted in larger  $d$ -spacing. This fact supports the enlargement in free volume observed for all **TR-PEBO** samples with regard to **HPEI** precursor, as  $d$ -spacing can be considered as an index of *openness* of the polymer matrix. On comparing the patterns of **TR-PEBO**, obtained from different treatment temperatures, it could be observed that samples thermally rearranged at 450 °C displayed an amorphous halo at 13.4° ( $2\theta$ ), that corresponds to a distance of 0.66 nm, whereas thermal rearrangement at 400 °C led to smaller augments in  $d$ -spacing (0.62–0.63 nm).

These results highlight that higher treatment temperatures result in lower chain packing density, as it was also mentioned above. However, as noticed from Figure 5, diverse heating times did not seem to show important differences in the average interchain distances of **TR-PEBO** membranes, in spite of the substantial effect in the density and FFV values, in particular for the membranes treated at 450 °C. Some authors observed a decrease in  $d$ -spacing with an increasing degree of thermal-cross-linking in the membrane or an important shift of the amorphous halo to larger theta angle values, indicative of an intermediate stage between polymer and carbon structure.<sup>20,22</sup> This was not the case for **TR-PEBO** membranes treated at 450 °C.

**Gas Transport Behaviors of TR-PEBO Membranes.** The gas permeabilities ( $P$ ) as well as the ideal separation factors for some interesting gas pairs of thermally rearranged and precursor polymer membranes are listed in Table 4. For comparative purposes, the permeability and ideal selectivities for related fluorinated polybenzoxazole (aPBO) from azeotropic hydroxyl–polyimide (6FDA-APAF), without any ether linkages,<sup>5</sup> have also been included. As previously described, solid-state rearrangement by heat treatment was shown to affect the topologies and the intrinsic properties of TR polymers, resulting in unusual increases in free volume elements as well as higher gas permeation properties.<sup>1–5</sup> Thus, precursor **HPEI** had very low permeability whereas **TR-PEBO** membranes showed enhanced gas permeabilities

**Table 4.** Gas Permeation Properties of Precursor Polyimide and Poly(ether–benzoxazole) Membranes

sample	gas permeability (Barrer) <sup>a</sup>						ideal selectivity <sup>b</sup>					
	He	H <sub>2</sub>	CO <sub>2</sub>	O <sub>2</sub>	N <sub>2</sub>	CH <sub>4</sub>	O <sub>2</sub> /N <sub>2</sub>	CO <sub>2</sub> /N <sub>2</sub>	CO <sub>2</sub> /CH <sub>4</sub>	H <sub>2</sub> /CO <sub>2</sub>	H <sub>2</sub> /CH <sub>4</sub>	N <sub>2</sub> /CH <sub>4</sub>
<b>HPEI</b>	42.1	29.1	8.6	1.9	0.46	0.13	4.1	18.7	66.2	3.4	223.8	3.5
<b>400-1</b>	70.7	59.5	23.3	6.2	1.02	0.62	6.1	22.8	37.6	2.6	96.0	1.6
<b>400-2</b>	74.9	64.5	27.0	10.7	1.98	1.35	5.4	13.6	20.0	2.4	47.8	1.5
<b>400-3</b>	61.7	51.2	22.5	5.6	1.52	0.80	3.7	14.8	28.1	2.3	64.0	1.9
<b>450-1</b>	101.1	95.3	41.4	10.0	1.89	1.45	5.3	21.9	28.6	2.3	65.7	1.3
<b>450-2</b>	145.2	158.1	118.6	23.1	5.50	3.90	4.2	21.6	30.4	1.3	40.5	1.4
<b>450-3</b>	317.7	439.0	485.8	88.5	20.0	17.0	4.4	24.3	28.6	0.9	25.8	1.2
aPBO	356	408	398	81	19	12	4.3	21	34	1.0	35	1.6

<sup>a</sup> 1 barrer = 10<sup>-10</sup> cm<sup>3</sup> (STP) cm/(s cm<sup>2</sup> cmHg). <sup>b</sup> Ideal selectivities were obtained by the ratio of two gas permeabilities.



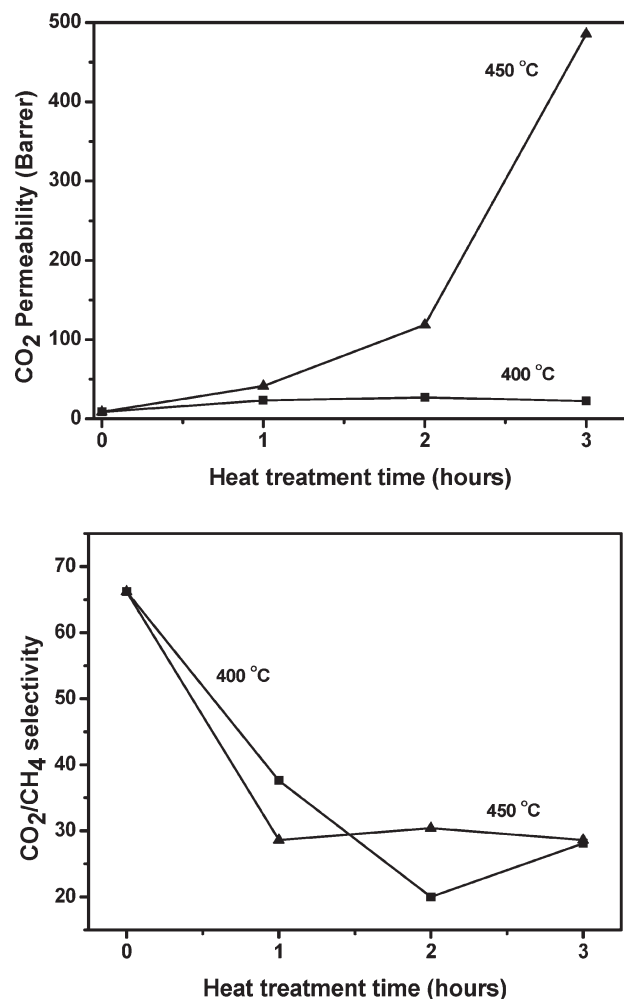


**Figure 6.** (a) CO<sub>2</sub> permeability and (b) CO<sub>2</sub>/CH<sub>4</sub> selectivity of **TR-PEBO** membranes treated at 400 and 450 °C as a function of heat treatment time.

due to the enlarged free volume elements. As expected by the density, FFV and the  $d$ -spacing, the increments in ( $P$ ) were greater when thermal rearrangement proceeded at 450 °C. As an example, Figure 6a exhibits the CO<sub>2</sub> permeability of **TR-PEBO** membranes and precursor polyimide treated at 400 and 450 °C as a function of heat treatment time.

Hence, thermal rearrangement at 400 °C roughly increased CO<sub>2</sub> permeability between 2.7 and 3 times where longer heating times, and so, higher degrees of conversion implied greater permeability, except for the 3 h treated sample (100% conversion), which showed a permeability decay due to its lower amount of fractional free volume (FFV), as discussed before. Nevertheless, at 450 °C the increments in CO<sub>2</sub> permeability were much greater, between 5 and 56 times while augmenting treatment time, correlating with the marked enlargement in FFV observed for these membranes. A similar trend was found for the rest of gases tested, that is, He, H<sub>2</sub>, O<sub>2</sub>, N<sub>2</sub>, and CH<sub>4</sub>. Thus, on analyzing the behavior of the **TR-PEBO** membranes treated at 450 °C against each gas in terms of thermal dwell time (Figure 7a), it could be noticed that  $P$  increased dramatically for the 3 h heated sample where the order was as follows: CO<sub>2</sub> > H<sub>2</sub> > He > O<sub>2</sub> > N<sub>2</sub> > CH<sub>4</sub>. In fact, precursor polyimide **HPEI** membrane showed higher H<sub>2</sub> permeability than CO<sub>2</sub> permeability, which is consistent with the order of increasing kinetic diameters of these penetrant molecules, but when increasing the treating

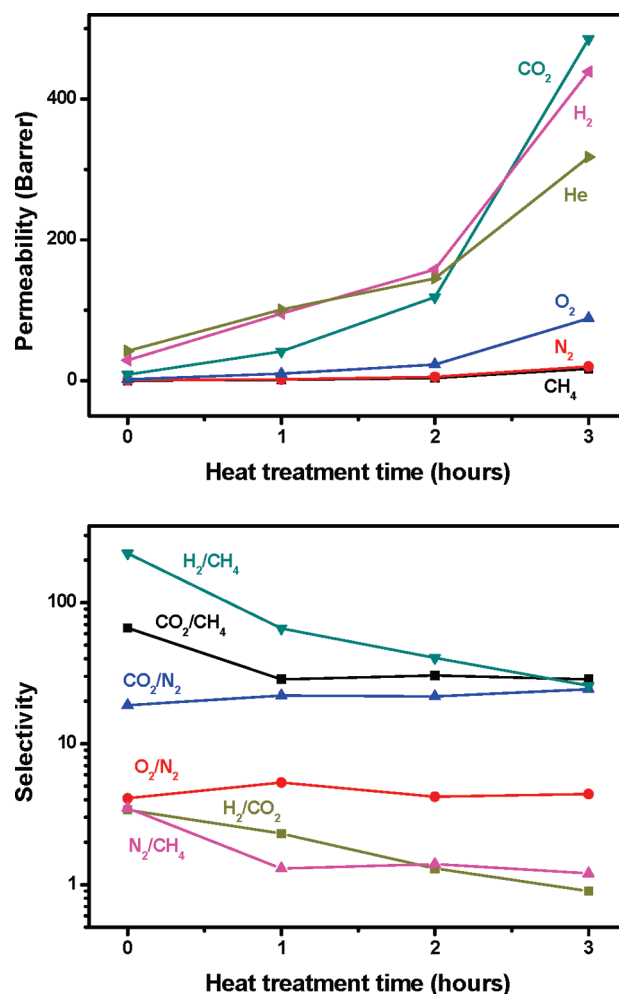


**Figure 7.** (a) Gas permeability and (b) gas selectivity of **TR-PEBO** membranes treated at 450 °C as a function of heat treatment time.

time, the differences between H<sub>2</sub> and CO<sub>2</sub> permeabilities were gradually reduced and finally, the order of  $P$  is changed for the 450–3 membrane. This behavior had been observed before in **TR** polymers,<sup>2</sup> and is due to the large fractional free volume of this **TR-PEBO** membrane, suggesting that much higher CO<sub>2</sub> solubility than H<sub>2</sub> solubility in this sample contributes to higher CO<sub>2</sub> permeability.

The gas selectivities (e.g., O<sub>2</sub>/N<sub>2</sub>, CO<sub>2</sub>/N<sub>2</sub>, CO<sub>2</sub>/CH<sub>4</sub>, H<sub>2</sub>/CO<sub>2</sub>, H<sub>2</sub>/CH<sub>4</sub>, N<sub>2</sub>/CH<sub>4</sub>) depended also strongly on heating protocol (Table 4). Figure 6b shows the CO<sub>2</sub>/CH<sub>4</sub> selectivity of **TR-PEBO** membranes treated at 400 and 450 °C. Thus, thermal conversion at 400 °C implied an important drop in the ideal CO<sub>2</sub>/CH<sub>4</sub> selectivity values by increasing treatment time except for sample 400–3, meaning exactly the opposite trend observed for the permeability coefficients. However, rearrangement from **HPEI** to **TR-PEBO** at 450 °C resulted in an initial higher decrease in the selectivity (about 2.3 times) which maintained almost constant on augmenting the heating time up to 2 and 3 h.

When looking at the different gas selectivities of the **TR-PEBO** membranes treated at 450 °C (Figure 7b), it can be noticed that most of them, that is, O<sub>2</sub>/N<sub>2</sub>, CO<sub>2</sub>/N<sub>2</sub>, CO<sub>2</sub>/CH<sub>4</sub>, and N<sub>2</sub>/CH<sub>4</sub>, remained steady or slightly changed when increasing heating time, whereas H<sub>2</sub>/CH<sub>4</sub> and H<sub>2</sub>/CO<sub>2</sub> selectivities progressively dropped; the permeability of the no condensable and small gas (H<sub>2</sub>) did not seem to increase as fast as the rest of the gases, in spite of its lowest kinetic



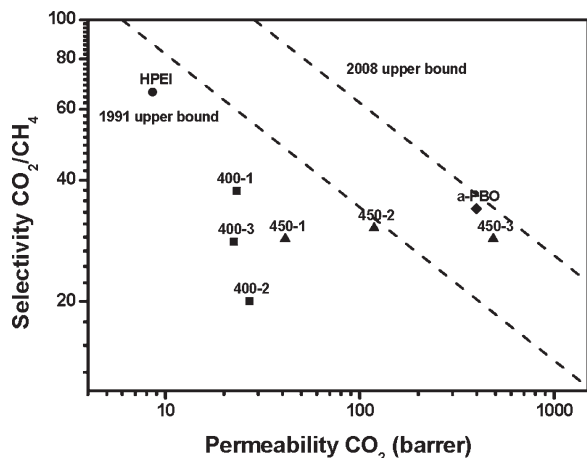


**Figure 8.** Relationship between  $\text{CO}_2$  permeability and  $\text{CO}_2/\text{CH}_4$  selectivity of HPEI and TR-PEBO membranes tested in this study with upper bounds.<sup>23,24</sup>

diameter (2.89 Å). As mentioned before, the thermal rearrangement at 450 °C brought about an increase in mean cavity size, and thus, in the permeability coefficients, but also on growing treating time this increase in cavity size seems to be accompanied by the coalescence of smaller cavities to form larger ones. This fact would explain the slower raise detected in the permeability of  $\text{H}_2$ , when compare with the other gases, and also the behavior observed in the ideal separation factors.

We also evaluated the permeability-selectivity relationship for the gas pairs studied. As an example, for the pair  $\text{CO}_2/\text{CH}_4$  (Figure 8), it can be observed that thermal rearrangement at 450 °C led to parallel increase of permeability with almost constant selectivity as a function of heating time. In particular, thermal rearrangement at 450 °C for 3 h moved transport properties across the previous Robeson's upper bound<sup>23</sup> and close to the 2008 upper bound.<sup>24</sup> Nevertheless, PEBO membranes thermally rearranged at 400 °C showed comparatively low performance in terms of permeability/selectivity trade-off because of the low conversion to PEBO and the resultant low fractional free volume elements.

On the other hand, from Table 4, it can be seen that gas permeabilities of reference TR polymer (aPBO), thermally rearranged at 450 °C for 1 h, were much higher than those of the analogous TR-PEBO 450–1 membrane, which is also in agreement with its higher FFV.<sup>5</sup> This fact supports that the introduction of ether linkages into the polybenzoxazole backbone, resulting in greater degree of rotational freedom and chain flexibility, prevents the evolution of micropores in TR-PBOs; it seems that the presence of bonds with unhindered rotation can cause the collapse of the microporous structure leading to much smaller gas permeabilities. As a matter of fact, the greater increments in permeability for TR-PEBO membranes thermally rearranged at 450 °C, when comparing with 400 °C treated ones, are presumably due to their much more cross-linked and rigid structure, preventing structural rearrangement that could result in the collapse of the porous structure.

## Conclusions

Novel poly(ether–benzoxazole) membranes have been synthesized by thermal rearrangement of an ether containing fluoro poly(hydroxy–imide). The introduction of ether linkages into the precursor polyimide backbone, resulting in greater degree of rotational freedom and chain flexibility, allows for rearrangement and decarboxylation to occur at faster rate and lower

temperature. Thus, full conversion to PEBO could be achieved efficiently at 400 °C, affording TR polybenzoxazole membranes with improved mechanical property, whereas thermal treatment at 450 °C speeded up the rate of conversion. However, this notable enhancement in the backbone flexibility seemed to prevent the evolution of free volume elements in TR-PBOs, resulting in much lower gas permeabilities. Thus, thermal rearrangement at 400 °C scarcely increased the permeability between 1.5 and 3 times for small gas molecules like He,  $\text{H}_2$ , and  $\text{CO}_2$ , whereas rearrangement at 450 °C brought about a higher enhancement in free volume elements, and thus, in the permeability coefficients on growing heating time. This fact is presumably due to the much more cross-linked and rigid structure for these membranes at 450 °C, as confirmed from the increased  $T_g$  values, preventing structural rearrangement that could result in the collapse of the porous structure.

From these results, it can be concluded that attainment of microporosity in TR polymers requires the TR process to be conducted at, near or below the  $T_g$ ; the development of nonequilibrium pore sizes is much more difficult to achieve when thermal rearrangement occurs above the  $T_g$ , leading to broader pore size distributions resulting in low molecular transport rates. The present study thus provides a more in-depth understanding and a meaningful insight into the structure–property relationship for TR polymer membranes, showing that chemical composition and moiety geometry, chain rigidity and physicochemical properties of hydroxy–polyimide precursors play major roles in determining the properties of the resultant TR polymer membranes, especially the micropore structure and separation capability.

**Acknowledgment.** This research was supported by the WCU (World Class University) program, National Research Foundation (NRF) of the Korean Ministry of Science and Technology (R31-10092), which we gratefully acknowledge.

## References and Notes

- (1) Park, H. B.; Jung, C. H.; Lee, Y. M.; Hill, A. J.; Pas, S. J.; Mudie, S. T.; Wagner, E. V.; Freeman, B. D.; Cookson, D. J. *Science* **2007**, *318*, 254.
- (2) Park, H. B.; Han, S. H.; Jung, C. H.; Lee, Y. M.; Hill, A. J. *J. Membr. Sci.* **2010**, *359*, 11.
- (3) Jung, C. H.; Lee, J. E.; Han, S. H.; Park, H. B.; Lee, Y. M. *J. Membr. Sci.* **2010**, *350*, 301.
- (4) Han, S. H.; Lee, J. E.; Lee, K. J.; Park, H. B.; Lee, Y. M. *J. Membr. Sci.* **2010**, *357*, 143.
- (5) Han, S. H.; Misdan, N.; Kim, S.; Doherty, C. M.; Hill, A. J.; Lee, Y. M. *Macromolecules* **2010**, *43*, 7657.
- (6) Hsiao, S. H.; Chiou, J. H. *J. Polym. Sci., Part A: Polym. Chem.* **2001**, *39*, 2262.
- (7) Hsiao, S. H.; He, M. H. *J. Polym. Sci., Part A: Polym. Chem.* **2001**, *39*, 4014.
- (8) Imai, Y.; Maeda, Y.; Takeuchi, H.; Park, K.-H.; Kakimoto, M.-A.; Kurosaki, T. *J. Polym. Sci., Part A: Polym. Chem.* **2002**, *40*, 2656.
- (9) Imai, Y.; Shibasaki, Y.; Takeuchi, H.; Park, K.-H.; Kakimoto, M.-A. *High Perform. Polym.* **2002**, *14*, 253.
- (10) Hsiao, S. H.; Chen, W.-T. *J. Polym. Sci., Part A: Polym. Chem.* **2003**, *41*, 914.
- (11) Hilborn, J. G.; Labadie, J. W.; Hedrick, J. L. *Macromolecules* **1990**, *23*, 2854.
- (12) Chern, Y. T. U.S. Patent 2006, 2006/0241187.
- (13) Choi, J. I.; Jung, C. H.; Han, S. H.; Park, H. B.; Lee, Y. M. *J. Membr. Sci.* **2010**, *349*, 358.
- (14) Tullios, G. L.; Mathias, L. J. *Polymer* **1999**, *40*, 3463.
- (15) Tullios, G. L.; Powers, J. M.; Jeskey, S. J.; Mathias, L. J. *Macromolecules* **1990**, *32*, 3598.
- (16) Barsena, J. N.; Klijnstra, S. D.; Balster, J. H.; van der Vegt, N. F. A.; Kooops, G. H.; Wessling, M. *J. Membr. Sci.* **2004**, *238*, 93.
- (17) Tanikella, R. V.; Sung, T.; Bidstrup-Allen, S. A.; Kohl, P. A. *IEEE Trans. Compon. Packag. Technol.* **2006**, *29*, 2.

- (18) Kim, T.-K.; Choi, K.-Y.; Lee, K.-S.; Park, D.-W.; Jin, M. Y. *Polym. Bullet.* **2000**, *44*, 55.
- (19) Shao, L.; Samseth, J.; Hagg, M. B. *Int. J. Greenhouse. Gas. Control.* **2008**, *2*, 492.
- (20) Xiao, Y.; Chung, T.-S.; *Energy Environ. Sci.*, **2010**, in press.
- (21) Park, J. Y.; Paul, D. R. *J. Membr. Sci.* **1997**, *125*, 23.
- (22) Shao, Lu.; Chung, T.-S.; Pramoda, K. P. *Microporous Mesoporous Mater.* **2005**, *84*, 59.
- (23) Robeson, L. M. *J. Membr. Sci.* **1991**, *62*, 165.
- (24) Robeson, L. M. *J. Membr. Sci.* **2008**, *320*, 390.